

# Phase interference effect in dissipative quantum tunneling

Xiao-Xiao Zhang<sup>1</sup> and Naoto Nagaosa<sup>2,3</sup>

<sup>1</sup>*Department of Physics and Astronomy & Stewart Blusson Quantum Matter Institute, University of British Columbia, Vancouver, BC, V6T 1Z4 Canada*

<sup>2</sup>*Department of Applied Physics, The University of Tokyo, 7-3-1 Hongo, Bunkyo-ku, Tokyo 113-8656, Japan*

<sup>3</sup>*RIKEN Center for Emergent Matter Science (CEMS), 2-1 Hirosawa, Wako, Saitama 351-0198, Japan*

We study in the presence of dissipation the quantum phenomena of tunneling and especially interference around a Weyl-like or conical potential crossing due to the monopolar Berry gauge phase. It is pertinent to a wide range of physical and quantum chemical phenomena, and we microscopically motivate this model from the effective dynamics of collective degrees of freedom arising from a two-level system coupled to a bosonic bath. Using the instanton approach with symmetry analysis and advanced numerical methods, we are able to investigate the interplay between phase interference and dissipation by resolving the phase diagram of coherent tunneling with respect to the potential bias and dissipation. Under emergent mirror symmetry protection, the coherent tunneling exhibits Kramers degeneracy, nonmonotonic dependence on dissipation and a generic phase transition to no interference, before which an anomalous dissipation-enhanced regime persists.

*Introduction.*— Quantum effects at the mesoscopic and macroscopic scales are a subject of theoretical and practical significance for it expands the subatomic realm of quantum mechanical phase coherence and rigidity that lay the foundation of many unique phenomena, from fermion/boson condensation to the ubiquitous Berry phase in semiclassical transport and topological materials[1–5]. Illustrated in Fig. 1, two prominent examples are the decay of a metastable state, macroscopic quantum tunnelling (MQT), and the coherent resonance in a degenerate two-minima system, macroscopic quantum coherence (MQC). They appear in Josephson junction systems[6–9], nanoscale magnetic grains or domains with collinear orders[10–12], and other systems[5, 9, 13]. Such systems inevitably are open and subject to decoherence and dissipation due to the influence from the omnipresent environmental degrees of freedom[14–17].

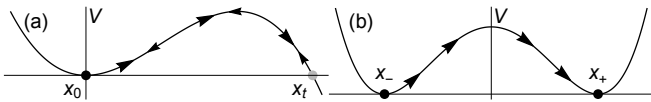


FIG. 1. Schematics of MQT and MQC in one dimension. (a) MQT instanton travels from the metastable  $x_0$  till  $x_t$  and turns back. (b) MQC instanton path connects two degenerate minima  $x_{\pm}$ .

An important question is how quantum geometric phases[18] and dissipation affect these phenomena *together*. In the system-plus-reservoir approach to quantum dissipative phenomena[6, 8, 16, 17], a powerful tool is, partly in line with the Heisenberg picture, semiclassically solving an effective action of the system of interest to the leading order of  $\hbar$ , the nonperturbative instanton technique[19]. Berry phase as the intrinsic leading quantum correction in  $\hbar$  can have nonnegligible association with instantons as being crucial, e.g., in quantum spin chains[20] and quantum magnetic phase transitions[21].

Because of the interference between distinct tunneling trajectories, suppression and oscillatory tunneling are possible[11, 12]. Aside, dissipation effect is often studied only in limiting cases as a perturbative or overdamped contribution[10, 22, 23] or numerically examined mostly for one-dimensional special potential forms[24, 25]. The quantum effects are usually reckoned to be suppressed by dissipation by arguing that the environment constantly measures and renders the system classical eventually, which usually does not properly incorporate phase interference together with dissipation.

Here, we aim to address this issue via a systematic way accounting for the phase and dissipation *at once*, especially focusing on the Berry gauge phase from a singular monopole structure in a three-dimensional (3D)  $\vec{Q}$ -variable space. Such a gauge phase proves to be the distinguishing feature responsible for a wide range of topological phenomena in real space as emergent magnetic monopoles[26] and in momentum space as band-crossing Weyl points[27]. The monopole enters our model as a two-level conical intersection and results in a potential landscape  $V(\vec{Q})$ . Because of the intimate relation between the dynamics of two-level system and monopole gauge field, we can motivate and derive our model from a variant of the spin-boson model, wherein the collective degree of freedom  $\vec{Q}$  couples to the spin fields and finally plays the role of instanton coordinate in the potential. Alternatively, this model could also come from the leading  $\hbar$ -expansion in the system's wave-packet dynamics[2] (henceforth  $\hbar = 1$ ). The conical potential intersection has partly its origin in the study of molecular physics and quantum chemistry[28]. It is the wavefunction phase singularity due to vibronic centrifugal terms of polyatomic molecules and brings about the wavefunction sign flip in Jahn-Teller systems[29, 30]. In the nonradiative energy or electron transfer processes in inorganic as well as photochemical reactions of organic molecules, the monopole

lar geometric phase can play a role at high collision energies to alter the reaction rate and scattering cross section[28, 31, 32]. Potential minima around an intersection form a typical reactive configuration, for which our study using the dissipative instanton with Berry phase can hopefully provide new insights.

*Model system.*– The motivation outlined above is embodied in the imaginary-time action

$$\begin{aligned} \mathcal{S}_{\text{tot}} = \mathcal{S}_{\Phi} + \mathcal{S}_{\text{Q}} = \mathcal{S}_{\Phi} + \int_{-T}^T d\tau \left[ \sum_i \frac{1}{2} M_i \dot{Q}_i^2(\tau) + V(\vec{Q}) \right. \\ \left. + \sum_i \int_{-T}^T d\tau' \frac{D_i}{4} \frac{(Q_i(\tau) - Q_i(\tau'))^2}{(\tau - \tau')^2} \right] \end{aligned} \quad (1)$$

that describes a reactive quasiparticle or collective mode  $\vec{Q} = (Q_1, Q_2, Q_3)$  with dissipative temporally nonlocal self-interaction, where mass  $M_i$  and dissipation strength  $D_i$  can in general be anisotropic. The quasiparticle feels a reversed potential  $-V(\vec{Q})$  with

$$V(\vec{Q}) = \sum_{i=1,2,3} (Q_i - w_i)^2 / \alpha_i - |\vec{Q}| \quad (2)$$

consisting of a harmonic confinement and the lower energy surface of a conical intersection at  $\vec{Q} = \vec{0}$ . Anisotropic  $\alpha_i$  and potential offset  $w_i$ , seen later, help form potential minima around the monopole (used interchangeably with conical intersection). The monopole Berry phase  $\Phi$  attached to the quasiparticle is

$$\mathcal{S}_{\Phi} = i\Phi = iS \int_{-T}^T d\tau (1 - \cos \theta) \dot{\phi} \quad (3)$$

with polar and azimuthal angles  $\theta, \phi$  in  $\vec{Q}$ -space, where  $S$  as a factor dependent on specific systems is spin- $\frac{1}{2}$  per the construction below.

Let's place a viable microscopic basis for this phenomenological model and keep corresponding quantities consistent to the above. We consider the Hamiltonian with a spin or two-level system  $H_s = \vec{w} \cdot \vec{\sigma}$  (spin- $\frac{1}{2}$  absorbed in  $w_i$ ) coupled to a group of harmonic oscillators  $H_b = \sum_{i\nu} \frac{m_{i\nu}}{2} (\dot{x}_{i\nu}^2 + \omega_{i\nu}^2 x_{i\nu}^2)$  labelled by  $\nu$  and direction  $i$

$$H = H_s + H_b + H_c. \quad (4)$$

In interaction  $H_c = \sum_i c_i \sigma_i q_i$  with coupling  $c_i$ , bosonic oscillators interact with spin via a collective coordinate  $q_i = \sum_{\nu} g_{i\nu} x_{i\nu}$  more of macroscopic nature and given by  $\{g_{i\nu}\}$  determined by the particular system. One can integrate out the boson fields except the collective mode  $\vec{q}$ , resulting in an effective action in Matsubara frequency  $\omega$ [33]

$$\mathcal{S}_{\text{eff}} = \mathcal{S}_s + 2T \sum_{i,\omega} (u_{i\omega}^{-1} q_{i\omega}^* q_{i\omega} + c_i \sigma_{i\omega}^* q_{i\omega}) \quad (5)$$

where the spin action  $\mathcal{S}_s = \mathcal{S}_{\Phi} + \int_{-T}^T d\tau H_s$  with spin Berry phase  $\mathcal{S}_{\Phi}$  in terms of Bloch-sphere angles formally identical to Eq. (3).  $u_{i\omega} = \frac{4}{\pi c_i^2} \int d\omega' J_i(\omega') \frac{\omega'}{\omega^2 + \omega'^2}$  with the coupling spectral density  $J_i(\omega)$ .  $J_i$  in reality differs from the memoryless ohmic friction  $J_0(\omega) = \eta\omega$  and decays fast enough as, for instance, an analytically tractable Lorentzian-like regularization does  $J_i(\omega) = \eta_i \omega / (1 + \omega^2 / \omega_D^2)^2$ , and acquires a memory-friction time scale  $1/\omega_D$  in the damping function. Henceforth, we make a coordinate transform to  $Q_i = w_i + c_i q_i$ , which places the monopole at the origin  $\vec{Q} = \vec{0}$  and simplifies discussions. Consequently, terms with  $M_i, D_i, \alpha_i$  in Eqs. (1)(2) are now generated from  $u$ -term in Eq. (5) as the leading contributions from integrating out the environment and should be treated independent in general. Since  $\vec{q}$  is the original coordinate, we set the generated  $\vec{q}$ -space quasiparticle mass, dissipation and harmonic potential isotropic for simplicity, leading to  $\vec{Q}$ -space  $M_i = \frac{1}{\alpha_i}, D_i = \frac{d}{\alpha_i}$  as all quantities are nondimensionalized and we have dimensionless potential parameters  $\vec{\alpha}, \vec{w}$  and dissipation  $d$ [33].

One also identifies a Hamiltonian  $H_0 = \vec{Q} \cdot \vec{\sigma}$  from the rest in Eq. (5). In accordance with Jahn-Teller potential energy surfaces, we take the adiabatic approximation as  $\vec{\sigma}$  inclines to follow the more macroscopic variable  $\vec{Q}$ [34].  $H_0$  is replaced by energy  $-|\vec{Q}|$  in Eq. (2) and  $\vec{Q}$  is manifestly the variable most relevant to the dynamics. Now the motion in  $\vec{Q}$  inherits the spin Berry phase, which we cast as  $\cos \theta = Q_3 / |\vec{Q}|, \dot{\phi} = (Q_1 \dot{Q}_2 - Q_2 \dot{Q}_1) / (Q_1^2 + Q_2^2)$ . The one-form  $\dot{\phi}$  facilitates evaluation since it is only singular along polar Dirac strings. The emergence of monopole phase or Weyl-like potential originates from that spin- $S$  bears the dynamics of a massless charge  $S$  under a monopole gauge field  $\vec{A}$ . In fact,  $\mathcal{S}_{\Phi}$  can be written as an orbital  $\vec{j} \cdot \vec{A}$ -type coupling  $iS \int_{\gamma} d\hat{n} \cdot \vec{A}$  where  $\hat{n} = \vec{S} / |\vec{S}|$  has trajectory  $\gamma$ . The mechanism lies in  $SU(2) \cong S^2 \times U(1)$  of spin  $SU(2)$  and monopole manifold  $S^2$ . Therefore, we are finally led to Eq. (1).

*Instanton equation and potential landscape.*– For Eq. (1), we will use the instanton technique to include the leading nonperturbative effect in the exponential contribution to the transition amplitude  $\langle \vec{Q}(T) | e^{-2\mathcal{H}T} | \vec{Q}(-T) \rangle = \int \mathcal{D}\vec{Q}(\tau) e^{-\mathcal{S}_{\text{tot}}[\vec{Q}(\tau)]}$  close to zero temperature with numerically large enough  $T$ . The fluctuation upon instantons that accounts for the less dominant non-exponential prefactor is not considered here. As per the adiabatic approximation and the original realness of the coordinate  $\vec{Q}$ , we solve the path for  $\mathcal{S}_{\text{Q}}$  while the imaginary  $\mathcal{S}_{\Phi}$  attaches a complex phase to the quantum amplitude. The instanton equation reads

$$M_i \frac{d^2 Q_i}{dx^2} - \frac{\partial V(\vec{Q})}{\partial Q_i} - D_i \int_{-T}^T d\tau' \frac{Q_i(\tau) - Q_i(\tau')}{(\tau - \tau')^2} = 0 \quad (6)$$

The boundary conditions (BCs) for MQT and MQC are respectively  $\vec{Q}(\pm T) = \vec{Q}_0$  and  $\vec{Q}(\pm T) = \vec{Q}_{\pm}$  where

	loss	gain
$\mathcal{S}_Q$	$\vec{Q}(\tau), V_h \rightarrow V_l$	$\mathcal{T}\vec{Q}(\tau), V_l \rightarrow V_h$
$\mathcal{S}'_Q (\geq \mathcal{S}_Q)$	$\mathcal{T}\vec{Q}'(\tau), V_l \rightarrow V_h$	$\vec{Q}'(\tau), V_h \rightarrow V_l$

TABLE I. Action and energy variation behavior of two solution paths  $\vec{Q}(\tau), \vec{Q}'(\tau)$  and their time-reversal connecting generic points  $\vec{Q}_{h,l}$ .

$V(\vec{Q}_0)$  is a metastable minimum and  $V(\vec{Q}_{\pm})$  are two degenerate minima. The anisotropy in  $\vec{\alpha}, \vec{w}$  and the mirror symmetry  $\mathcal{M}_i$  of  $V(\vec{Q})$  under  $Q_i \rightarrow -Q_i$  if  $w_i = 0$  can help create potentials with these features. To determine the extremum manifold given by  $\frac{\partial V(\vec{Q})}{\partial Q_i} = 0$ , we inspect principal minors of the Hessian  $\frac{\partial^2 V}{\partial Q_i \partial Q_j}$  [33]. As to be explained shortly, MQT instantons have no interference, we therefore mostly work on representative MQC cases assuming  $\alpha_1 > \alpha_2 > \alpha_3$ :  $\vec{w} = w_2\hat{2} + w_3\hat{3}$ ,  $\vec{Q}_{\pm} = (\pm\alpha_1\sqrt{\frac{1}{4} - \sum_{i=2,3} \frac{w_i^2}{(\alpha_1 - \alpha_i)^2}}, \frac{\alpha_1 w_2}{\alpha_1 - \alpha_2}, \frac{\alpha_1 w_3}{\alpha_1 - \alpha_3})$ , and its reduction when  $\vec{w} = w\hat{3}$  with condition  $\alpha_1 - \alpha_3 > 2w$ , illustrated in Fig. 2(a) inset.

We have a boundary-value problem (BVP) of a system of nonlinear integro-differential equations with a Fredholm integral, which in general lacks systematic treatment and possesses multiple solutions. Possible methods may include iteration, differential transform[35], Chebyshev decomposition[36], and asymptotic techniques[37]. However, the procedure could be uncontrolled or require exceeding computational cost towards correct convergence. Detailed in Supplemental Material (SM)[33], the essence of our efficient solution is, in the spirit of finite difference method (FDM)[36, 38], using irregular FDM stencils[39] generated from Gaussian quadrature rules[40] to convert simultaneously the differential and integral parts to a system of nonlinear algebraic equations, which can be solved by root-finding algorithms with initial guesses, e.g., Newton's and Brent's hybrid methods[41, 42]. Finer solutions are readily facilitated using any existing coarse and/or nearby-in-parameter solutions as initial warm-ups. This not only accelerates solutions but particularly helps reach symmetry-related instantons at will. All the properties discussed below are verified numerically in extensive parameter choices.

*Symmetry-related instantons.*— For a generic BVP of Eq. (6) connecting one higher and one lower points or local minima  $\vec{Q}_{h,l}$  with  $-V_h \leq -V_l$  in reversed potential, irrespective of MQT or MQC, one always finds two valid solutions:  $\vec{Q}(\tau)$  of globally minimal action  $\mathcal{S}_Q$  exhibits net energy loss and another  $\vec{Q}'(\tau)$  of locally minimal action  $\mathcal{S}'_Q \geq \mathcal{S}_Q$  exhibits net energy gain, since dissipating initial kinetic energy to travel  $\vec{Q}_h \rightarrow \vec{Q}_l$  is faster than gradually absorbing energy to accelerate. Seen more clearly in Table I, they are closely related to the time-reversed ( $\mathcal{T}$ ) paths of opposite energy variation that share the same  $\mathcal{S}_Q$  or  $\mathcal{S}'_Q$ . This situation is because al-

mirror symmetry	instanton	phase
$\mathcal{M}_1 : \vec{w} = w_2\hat{2} + w_3\hat{3}$	$\vec{Q}$	$\Phi$
	$\vec{Q}' = \mathcal{M}_1\mathcal{T}\vec{Q}$	$\Phi' = \Phi$
$\mathcal{M}_{1,2} : \vec{w} = w\hat{3}$	$\vec{Q}$	$\Phi$
	$\vec{Q}' = \mathcal{M}_1\mathcal{T}\vec{Q}$	$\Phi' = \Phi$
	$\vec{Q}^r = \mathcal{M}_2\vec{Q}$	$\Phi^r = -\Phi$
	$\vec{Q}^{r'} = \mathcal{M}_2\mathcal{M}_1\mathcal{T}\vec{Q}$	$\Phi^{r'} = -\Phi$

TABLE II. Valid instantons and associated phases related to a generic MQC instanton  $\vec{Q}(\tau)$  with phase  $\Phi$  depend on mirror symmetry conditions.

though the microscopic time-reversal symmetry  $\mathcal{S}$  is broken by Zeeman-like  $\vec{w}$  in Eq. (4), contrary to some common misconception, the  $\tau$ -reversibility  $\mathcal{T}$  in Eqs. (1)(4) remains intact. Temporally retarded or advanced self-interaction can both be induced from exchanging fluctuations with environment:  $\vec{Q}(\tau)$  and  $\mathcal{T}\vec{Q}(\tau) = \vec{Q}(-\tau)$  are both valid paths satisfying Eq. (6) (for different BCs) since the integro-differential operator is parity even, different from viscous Newtonian or Langevin equations that solely possess lossy solutions. In fact, any MQT instanton from a metastable  $\vec{Q}_0$ , unique or not, is  $\mathcal{T}$ -symmetric, i.e., opposite energy variation at  $\pm\tau$ , because the MQT instanton should comprise the two  $\mathcal{T}$ -related paths of the same minimal  $\mathcal{S}_Q$  in Table I as any MQT path must have two parts of interchanged BC. Therefore, loop paths encircling any flux are energetically unfavourable and as  $\mathcal{T}\vec{Q}(\tau)$  exactly retraces back  $\vec{Q}(\tau)$  and cancels phase accumulated, MQT instantons never enclose the monopole nor bear any interference, previously noted in the absence of dissipation[11]. The dissipative direction of time has to emerge from both densely distributed many-body states at thermodynamic limit due to environmental bath[43] and casual structure in subsystem's self-energy introduced by infinitesimal relaxation, which constitutes irreversibility in the same way as deriving Langevin-type equations via Matsubara or more general Keldysh formalism[44].

Let's henceforth focus on MQC that requires at least one emergent mirror symmetry in  $\vec{Q}$ -space as aforementioned and corresponds to the  $V_h = V_l, \mathcal{S}'_Q = \mathcal{S}_Q$  case of Table I. Readily verified in Eqs. (1)(3)(6) and accounting for the parity of the BCs  $Q_i(-T) = \pm Q_i(T)$ , we have at most three extra symmetry-related instantons of the same  $\mathcal{S}_Q[\vec{Q}(\tau)]$  as  $\vec{Q}$  does,  $\vec{Q}'$  aforementioned and a new  $\vec{Q}^r$  with its own  $\vec{Q}^{r'}$ , dependent on the number of mirror symmetries, summarized in Table II.  $\vec{Q}^r$  ( $\vec{Q}^{r'}$ ) does not contribute to any interference effect to  $\vec{Q}$  ( $\vec{Q}^r$ ) since they share the same phase, calculated from Eq. (3). Nonetheless, a reversed Berry phase  $\Phi^r = -\Phi$  and hence interference with  $\vec{Q}$  persists for  $\vec{Q}^r$  when  $\Phi \neq 0$ . Note that one cannot arbitrarily translate a system to accommodate  $Q_2(\pm T) = 0$  and obtain  $\vec{Q}^r$  since the two potentials in Eq. (2) have different inversion centers. Now the tran-

sition amplitude is

$$A_0 = 2(e^{-S_Q - S_\Phi} + e^{-S_Q^r - S_\Phi^r}) = 4e^{-S_Q} \cos \Phi \quad (7)$$

where the factor 2 originates from the  $\vec{Q}, \vec{Q}^r$  instantons in the sense that all four instantons of minimal action, however loss or gain, should be included in the path integral. As long as coherence persists, the probability of finding at one minimum oscillates at a frequency of the energy splitting,  $\Delta \propto A_0$  discussed later, between spontaneously formed even- and odd-parity states.

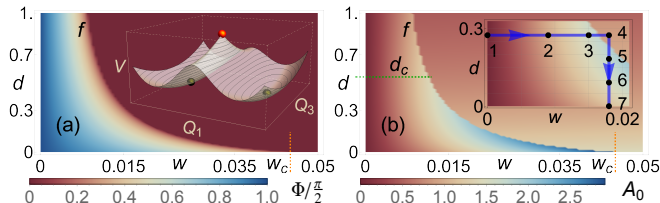


FIG. 2. Phase diagrams of MQC (a) instanton Berry phase  $\Phi$  and (b) coherent tunnel amplitude  $A_0$  against potential bias  $w$  and dissipation strength  $d$ . Phase boundary is the critical curve  $f$  where interference vanishes. Dashed lines: orange, maximal  $w_c$  with finite interference; green, maximal  $d_c$  of dissipation-enhanced  $A_0$ . Inset(a): potential landscape in the  $Q_1Q_3$ -plane at  $Q_2 = 0$  with two degenerate minima as black dots and the monopole as a red dot. Inset(b): seven points along the arrowed path are used in Fig. 3. Instantons are solved on a 200-point  $\tau$ -grid with parameters  $2T = 10, \vec{\alpha} = (1, 0.6, 0.4)$ , scanning a  $100 \times 100$ -mesh of the  $wd$ -plane.

*Kramers degeneracy, phase transition, and dissipation-enhanced MQC effect.*— We study the dependence of MQC phenomena on dissipation and potential bias  $\vec{w} = w\vec{3}$  for the interesting case with interference. In the whole  $w, d$ -plane, the action  $S_Q$  increases (decreases) with  $d$  ( $w$ ), as understood from the positive-definiteness of the nonlocal term in Eq. (1) and the longer instanton trajectory at smaller  $w$ . The former justifies the common belief of dissipation-suppressed MQT decay rate and MQC tunnel amplitude  $A_0$  or splitting  $\Delta$ . In Fig. 2(a), the phase  $\Phi$  decreases with  $w$ , ranging from full topological suppression at maximum  $\Phi = \pi/2$  on the  $w = 0$  line until vanishing along the phase boundary curve  $f$ , because larger  $w$  renders the instanton travelling higher above the monopole and thus acquiring less Berry phase as illustrated in Fig. 3(a). The MQC condition ends at  $w = (\alpha_1 - \alpha_3)/2$  (outside Fig. 2), the aforesaid brink of existence of two degenerate minima, much earlier than which we reach  $f$  at  $w_c$  when  $d = 0$ .

The variation of  $\Phi$  follows that of  $\max[|Q_2(\tau)|]$  for fixed finite  $w$  since  $Q_2$  is the mirror-symmetric direction responsible for expanding wider solid angle. Along  $w = 0$ , any dissipation that accommodates finite motion in  $Q_2$  gains full hemisphere covering of the monopole and hence  $\Phi = \pi/2$ . Recalling the microscopic model Eq. (4) with spin, this  $A_0 = 0$  partly reflects the original Kramers degeneracy as the aforesaid microscopic time-reversal  $\mathcal{T}$  is

not broken if  $w = 0$  and the two instantons interfere destructively [‘1’ in Fig. 3(a)]. Furthermore, a phase transition occurs across  $f$ , at which the topological phase  $\Phi$  continuously vanishes and is singular in its first derivative in Fig. 2(a) while in Fig. 2(b)  $A_0$  or  $\Delta$  discontinuously jumps downwards since  $\vec{Q}, \vec{Q}^r$  instantons merge into a single path and hence no phase interference outside  $f$ . Pictorially shown in Fig. 3(a), the  $\mathcal{M}_2$ -symmetric instanton pair forms at  $w = 0$  in the  $Q_1Q_2$ -plane a twin-leaf shape, and, as  $w$  increases, each leaf, in general in 3D due to the nonconservation of angular momentum from  $V$ , bends towards each other until coalescence at  $f$  into one single 2D leaf in  $Q_1Q_3$ -plane and remains outside  $f$ . More details and large- $d$  behavior are in the SM[33].

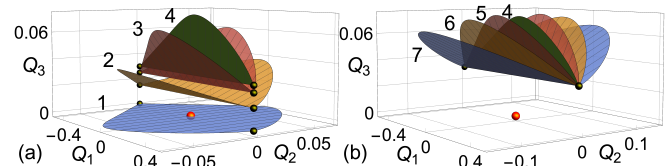


FIG. 3. Evolution of the  $\mathcal{M}_2$ -symmetry-related  $\vec{Q}(\tau), \vec{Q}^r(\tau)$  instanton pair along the path in Fig. 2(b) inset, which (a) increases  $w$  until case 4 outside the phase boundary (single green instanton) and then (b) decreases  $d$  to zero. Black and red dots are respectively two end points of instantons and the monopole or conical intersection.

A physically relevant region worth highlighting in Fig. 2(b) is from zero dissipation to  $d_c$ , mostly independent of  $w$ , and bounded by  $f$ , where  $A_0$  or  $\Delta$  is anomalously enhanced by increasing dissipation and in general goes much beyond the perturbative limit since  $d$  is well comparable to other parameters. Although the amplitude and phase effect bears a competition along the  $d$ -axis,  $A_0$  follows below  $d_c$  the effect of weakening topological suppression and thus results in this intriguing regime, which is a universal and robust feature against modification of parameters. The instanton evolution with  $d$  in Fig. 3(b) is qualitatively similar to the one with  $w$  in terms of approaching the phase transition. It is important to note that this is entirely different from the rare situation deemed experimentally mostly irrelevant, where dissipation does not inhibit tunneling as it is proportional to the squared rate of change of the conjugate momentum rather than the more common coordinate, related to the uncertainty principle[34, 45]. Here, we identify a more realistic scenario that does not require any anomalous type of coupling but relies on a generic interplay between the monopole gauge structure and the dissipation-dependent tunneling geometry, which cooperatively enhances the coherent tunnel amplitude.

*Dissipative instanton gas.*— The tunneling instantons can be generalized to a dissipative instanton gas with interference effect. In the gas picture, with all configurations of indefinite number of all

types of interfering instantons, the full transition amplitude from  $\vec{Q}_-$  to  $\vec{Q}_+$  or back to  $\vec{Q}_-$  is a grand-canonical partition function  $A(\vec{Q}_-, \vec{Q}_\mp) = \sum_{n=0}^{\infty} \int_{-T}^T d\tau_1 \int_{-T}^{\tau_1} d\tau_2 \cdots \int_{-T}^{\tau_{n+m-1}} d\tau_{n+m} y^{n+m} e^{-X}$  where  $m = n + \frac{1 \mp 1}{2}$ .  $X(\{\tau_i\}) = -c \sum_{i < j}^{n+m} q_i q_j \ln |\tau_i - \tau_j|$  accounts for the logarithmic Coulomb interaction due to dissipation in the dilute approximation with  $i$ th instanton's direction charge  $q_i = (-1)^{i+1}$ [46]. The gas fugacity from single instanton is calculated to be  $y = KA_0$  with  $K$  the harmonic fluctuation determinant. It is inapplicable to map this Coulomb gas to the sine-Gordon model due to the instanton time-ordering, while it formally resembles the anisotropic Kondo problem as per the two-state-flipping nature between  $\vec{Q}_\pm$ . From renormalization-group analysis[22, 33, 47], this inter-instanton nonlocal interaction leads to a critical dissipation  $d_c(w) = 2/[2Q_1(T)]^2 > 2$  in our case, i.e., the phase diagram region of interest is below the localization transition and the Toulouse limit: coherent or partially damped tunneling mostly remains valid. Here, we neglect the interaction's dependence on four instanton types, which is in principle possible and will otherwise lead to a more complex gas with the fugacity summation inseparable from interaction[33]. In the noninteracting limit,  $A(\vec{Q}_-, \vec{Q}_\mp) \propto \cosh(2KTA_0)$  or  $\sinh(2KTA_0)$ . Compared with the calculation from the even and odd ground-state subspace, the tunnel splitting  $\Delta = KA_0$ .

*Conclusion.*— We study the quantum tunneling and interference with both dissipation and monopole gauge phase associated with a conical potential intersection included simultaneously, which has its roots in various mesoscopic processes in solid-state and molecular physics and chemical reactions. A phenomenological model is derived from a microscopic picture and solved in a systematic approach taking the leading nonperturbative instanton effect into account. In the phase diagram, manifestation of Kramers degeneracy, phase transition to no interference and a regime of dissipation-enhanced MQC tunnelling are found, which also leads to a dissipative instanton gas with interference effect.

X.-X.Z appreciates stimulating discussions with K. Misaki. This work was supported by NSERC and CIFAR, JSPS Grant-in-Aids for Scientific Research (No. 26103006), CREST, Japan Science and Technology (Nos. JPMJCR16F1 & JPMJCR1874), and ImPACT Program of Council for Science, Technology and Innovation (Cabinet Office, Government of Japan, 888176).

- 
- [1] A. Bohm, A. Mostafazadeh, H. Koizumi, Q. Niu, and J. Zwanziger, *The Geometric Phase in Quantum Systems* (Springer Berlin Heidelberg, Heidelberg, 2003).  
 [2] D. Xiao, M.-C. Chang, and Q. Niu, *Reviews of Modern Physics* **82**, 1959 (2010).

- [3] M. Z. Hasan and C. L. Kane, *Rev. Mod. Phys.* **82**, 3045 (2010); X.-L. Qi and S.-C. Zhang, *Rev. Mod. Phys.* **83**, 1057 (2011).  
 [4] D. Xiao, G.-B. Liu, W. Feng, X. Xu, and W. Yao, *Physical Review Letters* **108**, 196802 (2012).  
 [5] F. Fröwis, P. Sekatski, W. Dür, N. Gisin, and N. Sangouard, *Reviews of Modern Physics* **90**, 025004 (2018).  
 [6] A. O. Caldeira and A. J. Leggett, *Phys. Rev. Lett.* **46**, 211 (1981); A. Caldeira and A. Leggett, *Ann. Phys.* **149**, 374 (1983).  
 [7] S. Chakravarty, *Physical Review Letters* **49**, 681 (1982).  
 [8] A. J. Leggett, S. Chakravarty, A. T. Dorsey, M. P. A. Fisher, A. Garg, and W. Zwerger, *Rev. Mod. Phys.* **59**, 1 (1987).  
 [9] P. C. E. Stamp, in *Proceedings from the Institute for Nuclear Theory* (World Scientific, Singapore, 1998) pp. 101–197; N. V. Prokof'ev and P. C. E. Stamp, *Rep. Prog. Phys.* **63**, 669 (2000).  
 [10] E. M. Chudnovsky and L. Gunther, *Phys. Rev. Lett.* **60**, 661 (1988); A. Garg and G.-H. Kim, *Phys. Rev. Lett.* **63**, 2512 (1989); *J. Appl. Phys.* **67**, 5669 (1990).  
 [11] A. Garg, *Europhysics Letters (EPL)* **22**, 205 (1993).  
 [12] D. Loss, D. P. DiVincenzo, and G. Grinstein, *Phys. Rev. Lett.* **69**, 3232 (1992); J. von Delft and C. L. Henley, *Phys. Rev. Lett.* **69**, 3236 (1992); H.-B. Braun and D. Loss, *Phys. Rev. B* **53**, 3237 (1996); A. Garg, *Phys. Rev. Lett.* **83**, 4385 (1999); M. N. Leuenberger and D. Loss, *Phys. Rev. B* **63**, 054414 (2001).  
 [13] A. Stern, Y. Aharonov, and Y. Imry, *Phys. Rev. A* **41**, 3436 (1990).  
 [14] W. H. Zurek, *Reviews of Modern Physics* **75**, 715 (2003).  
 [15] S. Dattagupta and S. Puri, *Dissipative Phenomena in Condensed Matter* (Springer Berlin Heidelberg, Heidelberg, 2004).  
 [16] U. Weiss, *Quantum Dissipative Systems* (World Scientific Publishing Company, Singapore, 2012).  
 [17] A. O. Caldeira, *An Introduction to Macroscopic Quantum Phenomena and Quantum Dissipation* (Cambridge University Press, Cambridge, 2014).  
 [18] M. V. Berry, *Proceedings of the Royal Society A: Mathematical, Physical and Engineering Sciences* **392**, 45 (1984); B. Simon, *Phys. Rev. Lett.* **51**, 2167 (1983).  
 [19] S. Coleman, *Phys. Rev. D* **15**, 2929 (1977); C. G. Callan and S. Coleman, *Phys. Rev. D* **16**, 1762 (1977); S. Coleman, *Aspects of Symmetry* (Cambridge University Press, Cambridge, 1985).  
 [20] I. Affleck, *Physical Review Letters* **56**, 408 (1986).  
 [21] N. Read and S. Sachdev, *Phys. Rev. Lett.* **62**, 1694 (1989); T. Senthil, A. Vishwanath, L. Balents, S. Sachdev, and M. P. A. Fisher, *Science* **303**, 1490 (2004).  
 [22] A. J. Bray and M. A. Moore, *Phys. Rev. Lett.* **49**, 1545 (1982).  
 [23] A. Garg, *Phys. Rev. Lett.* **70**, 1541 (1993); *J. Appl. Phys.* **76**, 6168 (1994).  
 [24] L.-D. Chang and S. Chakravarty, *Phys. Rev. B* **29**, 130 (1984).  
 [25] H. Grabert, P. Olschowski, and U. Weiss, *Phys. Rev. B* **36**, 1931 (1987).  
 [26] P. Goddard and D. I. Olive, *Rep. Prog. Phys.* **41**, 1357 (1978); C. Castelnovo, R. Moessner, and S. L. Sondhi, *Nature* **451**, 42 (2008); N. Nagaosa, X. Z. Yu, and Y. Tokura, *Philos. Trans. A: Math. Phys. Eng. Sci.* **370**, 5806 (2012); X.-X. Zhang, A. S. Mishchenko, G. De Fil-

- ippis, and N. Nagaosa, *Phys. Rev. B* **94**, 174428 (2016).
- [27] S. Murakami, *New J. Phys.* **9**, 356 (2007); X. Wan, A. M. Turner, A. Vishwanath, and S. Y. Savrasov, *Phys. Rev. B* **83**, 205101 (2011); N. P. Armitage, E. J. Mele, and A. Vishwanath, *Rev. Mod. Phys.* **90**, 015001 (2018).
- [28] D. R. Yarkony, *Reviews of Modern Physics* **68**, 985 (1996); W. Domcke, D. R. Yarkony, and H. Koppel, eds., *Conical Intersections: Electronic Structure, Dynamics and Spectroscopy* (World Scientific, Singapore, 2004).
- [29] G. Herzberg and H. C. Longuet-Higgins, *Discussions of the Faraday Society* **35**, 77 (1963); M. C. M. O'Brien, *Proceedings of the Royal Society of London. Series A. Mathematical and Physical Sciences* **281**, 323 (1964).
- [30] K. I. Kugel' and D. I. Khomskii, *Soviet Physics Uspekhi* **25**, 231 (1982).
- [31] D. L. Dexter, *The Journal of Chemical Physics* **21**, 836 (1953); T. Förster, *Discuss. Faraday Soc.* **27**, 7 (1959); G. C. Schatz and A. Kuppermann, *The Journal of Chemical Physics* **65**, 4668 (1976); C. A. Mead and D. G. Truhlar, *The Journal of Chemical Physics* **70**, 2284 (1979); Y.-S. M. Wu, A. Kuppermann, and B. Lepetit, *Chemical Physics Letters* **186**, 319 (1991).
- [32] M. Montalti, A. Credi, L. Prodi, and M. T. Gandolfi, *Handbook of Photochemistry* (CRC Press, Boca Raton, 2006).
- [33] See Supplemental Material for more details.
- [34] A. J. Leggett, in *Foundations of Quantum Mechanics in the Light of New Technology* (World Scientific, Singapore, 1997) pp. 406–413.
- [35] A. Arikoglu and I. Ozkol, *Applied Mathematics and Computation* **168**, 1145 (2005).
- [36] L. N. Trefethen, Á. Birkisson, and T. A. Driscoll, *Exploring ODEs* (SIAM-Society for Industrial and Applied Mathematics, Philadelphia, 2017).
- [37] J.-H. He, *International Journal of Modern Physics B* **20**, 1141 (2006).
- [38] R. J. LeVeque, *Finite Difference Methods for Ordinary and Partial Differential Equations* (SIAM-Society for Industrial and Applied Mathematics, Philadelphia, 2007).
- [39] B. Fornberg, *Mathematics of Computation* **51**, 699 (1988).
- [40] M. Abramowitz and I. Stegun, *Handbook of Mathematical Functions with Formulas, Graphs, and Mathematical Tables* (Martino Fine Books, Eastford, CT, 2014).
- [41] W. H. Press, S. A. Teukolsky, W. T. Vetterling, and B. P. Flannery, *Numerical Recipes: The Art of Scientific Computing*, 3rd ed. (Cambridge University Press, Cambridge, 2007).
- [42] B. Gough, ed., *GNU Scientific Library Reference Manual*, 3rd ed. (Network Theory Ltd., Bristol, 2009).
- [43] S. Datta, *Quantum Transport: Atom to Transistor* (Cambridge University Press, Cambridge, 2005).
- [44] A. Kamenev, *Field Theory of Non-Equilibrium Systems* (Cambridge University Press, Cambridge, 2009).
- [45] A. J. Leggett, *Phys. Rev. B* **30**, 1208 (1984); A. Widom and T. D. Clark, *Phys. Rev. B* **30**, 1205 (1984).
- [46] A. Schmid, *Phys. Rev. Lett.* **51**, 1506 (1983).
- [47] P. W. Anderson and G. Yuval, *Journal of Physics C: Solid State Physics* **4**, 607 (1971).
- [48] A. A. Soluyanov, D. Gresch, Z. Wang, Q. Wu, M. Troyer, X. Dai, and B. A. Bernevig, *Nature* **527**, 495 (2015).
- [49] K. Misaki and N. Nagaosa, *Physical Review E* **98**, 052225 (2018).
- [50] G. H. Golub and J. H. Welsch, *Mathematics of Computation* **23**, 221 (1969).
- [51] D. P. Laurie, in *Applications and Computation of Orthogonal Polynomials* (Birkhuser Basel, Basel, 1999) pp. 133–144.
- [52] A. Garg and G.-H. Kim, *Phys. Rev. B* **45**, 12921 (1992).
- [53] A. Altland and B. D. Simons, *Condensed Matter Field Theory*, 2nd ed. (Cambridge University Press, Cambridge, 2010).

# Supplemental Material for “Phase interference effect in dissipative quantum tunneling”

## CONTENTS

I. Derivation of effective Lagrangian and instanton equation	1
II. Instanton potential landscape	4
III. Details in symmetry analysis	5
A. Time-reversed solutions	5
B. Mirror symmetry protection	6
IV. Numerical method	6
V. Analytical analysis of instanton solutions	7
VI. Dissipative instanton gas tunnelling	9

### I. DERIVATION OF EFFECTIVE LAGRANGIAN AND INSTANTON EQUATION

We consider the Hamiltonian with a single spin- $\frac{1}{2}$  or any two-level system coupled to a group of bosonic fields

$$H = H_s + H_b + H_c + H_{ct}. \quad (S1)$$

For completeness, we also include the counter term  $H_{ct} = \sum_{i\nu} \frac{\tilde{c}_{i\nu}^2}{2m_\nu\omega_\nu^2} \sigma_i \sigma_i$  with  $\tilde{c}_{i\nu} = c_i g_{i\nu}$ .  $H_{ct}$  compensates the side effect of  $H_c$  and retains the original potential surface of  $H_s$ , without which  $H_c$  introduces not only dissipation. However, for the two-level nature,  $H_{ct}$  herein becomes constant and insignificant and is neglected in the main text. We work in the imaginary time formalism with  $t \rightarrow -i\tau$  and hence  $e^{iS/\hbar} \rightarrow e^{-S/\hbar}$  for any action  $S$  and we use the Fourier convention  $\varphi(\tau) = \sum_\omega e^{-i\omega\tau} \varphi_\omega$  and  $\varphi_\omega = \frac{1}{\beta} \int_0^\beta d\tau \varphi(\tau) e^{i\omega\tau}$  where  $\omega$  stands for generic bosonic Matsubara frequencies and we for the nonce set  $\tau \in [0, \beta]$  in compliance with the common notation. The corresponding actions are the following ones.

$$\mathcal{S}_s = \mathcal{S}_\Phi + \int_0^\beta d\tau H_s. \quad (S2)$$

where we include the spin Berry phase term

$$\mathcal{S}_\Phi = i\Phi = iS \int_0^\beta d\tau (1 - \cos\theta) \dot{\phi} \quad (S3)$$

with polar and azimuthal angle  $\theta, \phi$  on the Bloch sphere of the spin  $S$ .

$$\mathcal{S}_b = \int_0^\beta d\tau \sum_{i\nu} \frac{m_\nu}{2} (\dot{x}_{i\nu}^2 + \omega_\nu^2 x_{i\nu}^2) = \beta \sum_{i\nu} \frac{m_\nu}{2} \sum_\omega (\omega^2 + \omega_\nu^2) x_{i\nu\omega}^i x_{i\nu,-\omega}^i. \quad (S4)$$

$$\mathcal{S}_c = \int_0^\beta d\tau \sum_i c_i \sigma_i q_i = \beta \sum_{i\omega} c_i \sigma_{i\omega} q_{i,-\omega} = \beta \sum_{i\nu\omega} \tilde{c}_{i\nu} \sigma_{i\omega} x_{i\nu,-\omega}. \quad (S5)$$

$$\mathcal{S}_{ct} = \int_0^\beta d\tau \sum_{i\nu} \frac{\tilde{c}_{i\nu}^2}{2m_\nu\omega_\nu^2} \sigma_i(\tau) \sigma_i(\tau) = \beta \sum_{i\nu\omega} \frac{\tilde{c}_{i\nu}^2}{2m_\nu\omega_\nu^2} \sigma_{i\omega} \sigma_{i,-\omega}. \quad (S6)$$

And we introduce the Lagrange multiplier  $\lambda_i$  for the collective coordinate  $\vec{q}$

$$\mathcal{S}_\lambda = \int_0^\beta d\tau \sum_i i\lambda_i(\tau)(q_i(\tau) - \sum_\nu g_{i\nu}x_{i\nu}) = i\beta \sum_{i\omega} \lambda_{i\omega}(q_{i,-\omega} - \sum_\nu g_{i,\nu}x_{i\nu,-\omega}). \quad (\text{S7})$$

We integrate out all the bosonic bath in the partition function except the collective modes  $q_i$

$$\begin{aligned} \mathcal{Z}[\sigma, x, q, \lambda] &= \int \mathcal{D}\sigma \mathcal{D}x \mathcal{D}q \mathcal{D}\lambda e^{-(\mathcal{S}_s + \mathcal{S}_b + \mathcal{S}_c + \mathcal{S}_{ct} + \mathcal{S}_\lambda)} \\ &= \int \mathcal{D}\sigma \mathcal{D}x \mathcal{D}q \mathcal{D}\lambda e^{-(\mathcal{S}_s + \mathcal{S}_{ct} + \beta \sum_{i\nu\omega} \{ \frac{m_\nu}{2}(\omega^2 + \omega_\nu^2)x_{i\nu\omega}^* x_{i\nu\omega} + (\tilde{c}_{i\nu}\sigma_{i\omega}^* - ig_{i\nu}\lambda_{i\omega}^*)x_{i\nu\omega} \} + i\beta \sum_{i\omega} \lambda_{i\omega} q_{i,-\omega})} \\ &= \mathcal{Z}_x \int \mathcal{D}\sigma \mathcal{D}q \mathcal{D}\lambda e^{-(\mathcal{S}_s + \mathcal{S}_{ct} + \beta \sum_{i\nu\omega} (-B_{\nu\omega})(\tilde{c}_{i\nu}\sigma_{i\omega}^* - ig_{i\nu}\lambda_{i\omega}^*)(\tilde{c}_{i\nu}\sigma_{i\omega} - ig_{i\nu}\lambda_{i\omega}) + i\beta \sum_{i\omega} \lambda_{i\omega} q_{i,-\omega})} \\ &= \mathcal{Z}_x \int \mathcal{D}\sigma \mathcal{D}q \mathcal{D}\lambda e^{-(\mathcal{S}_s + \mathcal{S}_{ct} + \beta \sum_{i\omega} \{ -w_{i\omega}\sigma_{i\omega}^*\sigma_{i\omega} + \frac{1}{4}u_{i\omega}\lambda_{i\omega}^*\lambda_{i\omega} + i[\lambda_{i\omega}^*(\frac{1}{2}q_{i\omega} + v_{i\omega}\sigma_{i\omega}) + (\frac{1}{2}q_{i\omega}^* + v_{i\omega}\sigma_{i\omega}^*)\lambda_{i\omega}] \})} \quad (\text{S8}) \\ &= \mathcal{Z}_{x\lambda} \int \mathcal{D}\sigma \mathcal{D}q e^{-(\mathcal{S}_s + \mathcal{S}_{ct} + \beta \sum_{i\omega} [-w_{i\omega}\sigma_{i\omega}^*\sigma_{i\omega} + 4u_{i\omega}^{-1}(\frac{1}{2}q_{i\omega} + v_{i\omega}\sigma_{i\omega})(\frac{1}{2}q_{i\omega}^* + v_{i\omega}\sigma_{i\omega}^*)])} \\ &= \mathcal{Z}_{x\lambda} \int \mathcal{D}\sigma \mathcal{D}q e^{-(\mathcal{S}_s + \mathcal{S}_{ct} + \beta \sum_{i\omega} [u_{i\omega}^{-1}q_{i\omega}^*q_{i\omega} + c_i(\sigma_{i\omega}^*q_{i\omega} + q_{i\omega}^*\sigma_{i\omega})/2])} \\ &= \mathcal{Z}_{x\lambda q} \int \mathcal{D}\sigma \mathcal{D}q e^{-(\mathcal{S}_s + \mathcal{S}_{ct} + \beta \sum_{i\omega} (-w_{i\omega}\sigma_{i\omega}^*\sigma_{i\omega}))} \end{aligned}$$

where we introduce for the sake of notational brevity  $A_i = \sum_\nu \frac{\tilde{c}_{i\nu}^2}{2m_\nu\omega_\nu^2}$ ,  $B_{\nu\omega} = \frac{1}{2m_\nu(\omega^2 + \omega_\nu^2)}$ ,  $u_{i\omega} = 4\sum_\nu B_{\nu\omega}g_{i\nu}^2$ ,  $w_{i\omega} = \sum_\nu B_{\nu\omega}\tilde{c}_{i\nu}^2 = c_i^2u_{i\omega}/4$ ,  $v_{i\omega} = \sum_\nu B_{\nu\omega}g_{i\nu}\tilde{c}_{i\nu} = c_iu_{i\omega}/4$  and absorb the generated determinants into the prefactors. From the penultimate line of Eq. (S8), we obtain the effective action  $\mathcal{S}_{\text{eff}}$  for the spin system coupled to the collective mode  $\vec{q}$

$$\mathcal{S}_{\text{eff}} = \mathcal{S}_s + \beta \sum_{i\omega} [u_{i\omega}^{-1}q_{i\omega}^*q_{i\omega} + c_i\sigma_{i\omega}^*q_{i\omega} + A_i\sigma_{i\omega}^*\sigma_{i\omega}] = \mathcal{S}_s + \mathcal{S}_D + \mathcal{S}_c + \mathcal{S}_{ct} \quad (\text{S9})$$

where

$$\mathcal{S}_D = \frac{1}{\beta} \sum_i \int_0^\beta d\tau d\tau' u_i^{-1}(\tau - \tau')q_i(\tau)q_i(\tau') \quad (\text{S10})$$

is the newly generated temporally nonlocal interaction responsible for dissipation. And also we have the pure spin effective action  $\mathcal{S}'_{\text{eff}}$  from the last line of Eq. (S8) where the counter term  $\mathcal{S}_{ct}$  cancels partially the action

$$\mathcal{S}'_{\text{eff}} = \mathcal{S}_s + \beta \sum_{i\nu\omega} \frac{\tilde{c}_{i\nu}^2}{2m_\nu\omega_\nu^2(\omega^2 + \omega_\nu^2)} \sigma_{i\omega}^*\sigma_{i\omega} = \mathcal{S}_s + \mathcal{S}_i, \quad (\text{S11})$$

where

$$\mathcal{S}_i = \frac{1}{\beta} \int_0^\beta d\tau d\tau' \sum_i \sigma_i(\tau)\sigma_i(\tau')K_i(\tau - \tau') \quad (\text{S12})$$

is the interaction term nonlocal in time,

$$K_i(\tau) = \int_0^\infty \frac{d\omega'}{\pi} J_i(\omega')D_{\omega'}(\tau) \quad (\text{S13})$$

is the temporally nonlocal kernel,

$$J_i(\omega) = \frac{\pi}{2} \sum_\nu \frac{\tilde{c}_{i\nu}^2}{m_\nu\omega_\nu} \delta(\omega - \omega_\nu) \quad (\text{S14})$$

is the spectral density of the coupling to the bosonic environment and  $D_{\omega'}(\tau) = \sum_\omega \frac{\omega^2}{\omega'(\omega^2 + \omega'^2)} e^{i\omega\tau}$ .

In reality, the spectral density  $J_i$  in Eq. (S14) must differ from the ideal memoryless friction of  $J_0(\omega) = \eta\omega$  and decay fast enough as  $\omega \rightarrow \infty$ . Here we adopt an analytically tractable Lorentzian-like regularization with cutoff frequency  $\omega_D$

$$J_i(\omega) = \eta_i \omega^s / (1 + \omega^2/\omega_D^2)^2 \quad (\text{S15})$$

and the corresponding memory-friction kernel  $\gamma(\omega)$ , also known as the damping function in the generalized Langevin equation, will acquire a memory-friction time scale  $1/\omega_D$ . The low-frequency behavior does not depend on the specific regularization form as long as the decay is fast enough. Then  $A_i = \frac{1}{\pi} \int \frac{d\omega}{\omega} J_i(\omega)$  and when  $s < 4$

$$u_{i\omega} = \frac{4}{\pi c_i^2} \int d\omega' J_i(\omega') \frac{\omega'}{\omega^2 + \omega'^2} = \frac{\eta_i \omega_D^2 [\omega_D^s (\omega^2 s + (2-s)\omega_D^2) - 2\omega_D^2 |\omega^s|]}{c_i^2 (\omega^2 - \omega_D^2)^2} \csc \frac{\pi s}{2}. \quad (\text{S16})$$

For the ohmic dissipation  $s = 1$ , we have  $u_{i\omega} = \frac{\eta_i}{\pi c_i^2} \frac{\pi \omega_D^3}{(\omega_D + |\omega|)^2}$  and  $A_i = \eta_i \omega_D / 4$ . Henceforth, we will set  $\eta_i = \eta$  for simplicity and  $\mathcal{S}_{ct}$  becomes an insignificant constant in the coherent state spin path integral. In the following, let's study the kernel  $X_{i\omega} = (u_{i\omega})^{-1} = \frac{\kappa_i}{\omega_D^2} (\omega_D^2 + 2\omega_D |\omega| + \omega^2)$  that appears in Eq. (S9) and we denote  $\kappa_i = \frac{c_i^2}{\eta_i \omega_D}$ . In the imaginary-time domain, we have

$$X_i(\tau, \tau') = \beta \kappa_i \delta(\tau - \tau') + K_i^*(\tau - \tau') + \frac{\kappa_i}{\omega_D^2} \partial_\tau \partial_{\tau'} \delta(\tau - \tau') \quad (\text{S17})$$

where  $K_i^*(\tau) = \frac{2\kappa_i}{\omega_D} \mathcal{F}[|\omega|]$  and  $\mathcal{F}$  means the Fourier transform. We digress a little on the evaluation of  $K_i^*$  and consider a general  $k(\tau) = \frac{\xi}{2} \mathcal{F}[|\omega|]$ . We express the Fourier component of  $k(\tau)$ ,  $k_n = \frac{\xi}{2} |\omega_n|$ , by introducing a spectral density  $J(\omega) = \xi\omega$  and follow the summation form in Eqs. (S13)(S14)

$$k_n = \sum_\nu \frac{c_\nu^2}{2m_\nu \omega_\nu^2} \frac{\omega_n^2}{\omega_\nu^2 + \omega_n^2} = \frac{\xi}{2} |\omega_n| = \frac{\omega_n^2}{\pi} \int_0^\infty d\omega \frac{J(\omega)}{\omega(\omega^2 + \omega_n^2)} \quad (\text{S18})$$

where we restore the Matsubara index  $n$  for clearness. Then we have the following properties: 1) Because of  $k_n = k_{-n}$  we have  $k(\tau) = k(\beta - \tau)$ ; 2) The 0th Fourier component  $\frac{1}{\beta} \int_0^\beta d\tau k(\tau) = k_{n=0} = 0$ ; 3) We can define  $K(\tau) = \beta \zeta \delta(\tau) - k(\tau)$  where  $\zeta = \sum_\nu \frac{c_\nu^2}{2m_\nu \omega_\nu^2} = \frac{1}{\pi} \int_0^\beta d\omega \frac{J(\omega)}{\omega}$ ; 4)  $K_n = \zeta - k_n = \sum_\nu \frac{c_\nu^2}{2m_\nu (\omega_\nu^2 + \omega_n^2)} = \frac{1}{\pi} \int_0^\beta d\omega \frac{J(\omega)\omega}{\omega^2 + \omega_n^2}$ . We can thus obtain

$$\begin{aligned} \beta \sum_{\omega_n} k_n q_n^* q_n &= \frac{1}{\beta} \int_0^\beta d\tau d\tau' k(\tau - \tau') q_i(\tau) q_i(\tau') \stackrel{1)}{=} \frac{2}{\beta} \int_0^\beta d\tau \int_0^\tau d\tau' k(\tau - \tau') q_i(\tau) q_i(\tau') \\ &\stackrel{2)}{=} -\frac{1}{\beta} \int_0^\beta d\tau \int_0^\tau d\tau' k(\tau - \tau') (q_i(\tau) - q_i(\tau'))^2 \stackrel{3)}{=} \frac{1}{\beta} \int_0^\beta d\tau \int_0^\tau d\tau' K(\tau - \tau') (q_i(\tau) - q_i(\tau'))^2. \end{aligned} \quad (\text{S19})$$

$$K(\tau) = \sum_n K_n e^{i\omega_n \tau} \stackrel{4)}{=} \frac{\beta}{2\pi} \int_0^\beta d\omega J(\omega) \frac{\cosh[\omega(\beta/2 - \tau)]}{\sinh(\omega\beta/2)} = \xi \frac{\beta}{2\pi} \frac{(\pi/\beta)^2}{\sin^2(\pi\tau/\beta)}. \quad (\text{S20})$$

Therefore,  $\mathcal{F}[|\omega|] = \frac{2}{\xi} \beta \zeta \delta(\tau) - \frac{\beta}{\pi} \frac{(\pi/\beta)^2}{\sin^2(\pi\tau/\beta)}$ . When  $\tau \ll \beta$  as required by our focus of the zero-temperature case, we can make the replacement  $\frac{\pi}{\beta^2} \frac{1}{\sin^2[\pi(\tau - \tau')/\beta]} \rightarrow \frac{1}{\pi} \frac{1}{(\tau - \tau')^2}$ . And our effective action becomes

$$\mathcal{S}_{\text{tot}} = \mathcal{S}_\Phi + \int_0^\beta d\tau \left[ \sum_i \frac{1}{2} m_i \dot{q}_i^2(\tau) + V(\vec{q}) + \sum_i \int_0^\beta d\tau' \frac{d_i}{4} \frac{(q_i(\tau) - q_i(\tau'))^2}{(\tau - \tau')^2} \right]. \quad (\text{S21})$$

where  $m_i = \frac{2\kappa_i}{\omega_D^2}$ ,  $d_i = \frac{4\kappa_i}{\pi\omega_D}$ ,  $\mu_i = \kappa_i$ ,  $V(\vec{q}) = -|\vec{Q}| + \sum_i \mu_i q_i^2(\tau)$ . Here  $m_i, d_i, \mu_i$  apparently have two degrees of freedom. It is important to note that this is merely an artifact of the simple form of regularization in Eq. (S15). In general, those three parameters are independent and are the leading terms generated from integrating out the environment. Henceforth, we will treat them as free parameters.

For the sake of later instanton solutions under general BCs, we note that  $\beta$  should be replaced by an imaginary time  $2T$  not necessarily related to temperature, since we are actually calculating the transition amplitude from the initial position  $\vec{Q}^i$  to the final position  $\vec{Q}^f$  in imaginary time  $[-T, T]$

$$\langle \vec{Q}^f | e^{-2\mathcal{H}T} | \vec{Q}^i \rangle = \int_{\vec{Q}(-T)=\vec{Q}^i}^{\vec{Q}(T)=\vec{Q}^f} \mathcal{D}\vec{Q}(\tau) e^{-S[\vec{Q}(\tau)]}, \quad (\text{S22})$$

which takes the form of a partition function. Let us now change the variable to  $\vec{Q}$  and nondimensionalize  $\mathcal{S}_Q$  in the total action Eq. (S21)  $\mathcal{S} = \mathcal{S}_\Phi + \mathcal{S}_Q$

$$\begin{aligned} \mathcal{S}_Q &= \int_{-T}^T d\tau \left[ \sum_i \frac{m_i}{2c_i^2} \dot{Q}_i^2 + V(\vec{Q}) \right] + \int_{-T}^T \int_{-T}^T d\tau d\tau' \sum_i \frac{d_i}{4c_i^2} \frac{(Q_{i\tau} - Q_{i\tau'})^2}{(\tau - \tau')^2} \\ &= \int_{-\tilde{T}}^{\tilde{T}} d\tilde{\tau} \left[ \sum_i \frac{m_i}{2c_i^2 \tau_0} \left( \frac{dQ_i}{d\tilde{\tau}} \right)^2 + \tau_0 V(\vec{Q}) \right] + \int_{-\tilde{T}}^{\tilde{T}} \int_{-\tilde{T}}^{\tilde{T}} d\tilde{\tau} d\tilde{\tau}' \sum_i \frac{d_i}{4c_i^2} \frac{(Q_{i\tilde{\tau}} - Q_{i\tilde{\tau}'})^2}{(\tilde{\tau} - \tilde{\tau}')^2} \\ &= \alpha_0 \tau_0 \left( \int_{-\tilde{T}}^{\tilde{T}} d\tilde{\tau} \left[ \sum_i \frac{\tilde{m}_i}{2} \left( \frac{d\tilde{Q}_i}{d\tilde{\tau}} \right)^2 + \tilde{V}(\vec{\tilde{Q}}) \right] + \int_{-\tilde{T}}^{\tilde{T}} \int_{-\tilde{T}}^{\tilde{T}} d\tilde{\tau} d\tilde{\tau}' \sum_i \frac{\tilde{d}_i}{4} \frac{(\tilde{Q}_{i\tilde{\tau}} - \tilde{Q}_{i\tilde{\tau}'})^2}{(\tilde{\tau} - \tilde{\tau}')^2} \right) \end{aligned} \quad (\text{S23})$$

where

$$\tilde{V}(\vec{\tilde{Q}}) = \sum_i (\tilde{Q}_i - \tilde{w}_i)^2 / \tilde{\alpha}_i - |\vec{\tilde{Q}}| \quad (\text{S24})$$

and we introduce  $\alpha_i = c_i^2 / \mu_i$ . All dimensional quantities are nondimensionalized as the following  $\tilde{\alpha}_i = \alpha_i / \alpha_0$ ,  $\tilde{w}_i = w_i / \alpha_0$ ,  $\tilde{Q}_i = Q_i / \alpha_0$ ,  $\tilde{m}_i = \frac{m_i}{m_0 c_i^2}$ ,  $\tilde{\tau} = \tau / \tau_0$ ,  $\tilde{T} = T / \tau_0$ ,  $\tilde{c}_i = c_i / \sqrt{\alpha_0 \mu_0}$ ,  $\tilde{d}_i = \frac{d_i}{c_i^2 \sqrt{m_0 \mu_0}}$  with  $\tau_0 = \sqrt{m_0 / \mu_0}$ . Therefore, one needs to choose three dimensional base parameters  $\alpha_0, m_0, \mu_0$  in total. As per the adiabatic approximation and the original realness of the coordinate  $\vec{Q}$ , we proceed by solving the path for the real-valued  $\mathcal{S}_Q$  while the imaginary  $\mathcal{S}_\Phi$  solely attaches a complex phase to the quantum amplitude. The instanton Euler-Lagrange semiclassical equation of motion (EOM)  $\frac{\delta \mathcal{S}_Q}{\delta \vec{Q}_i} = 0$  takes the form

$$\tilde{m}_i \frac{d^2 \tilde{Q}_i}{d\tilde{\tau}^2} - \frac{\partial \tilde{V}(\vec{\tilde{Q}})}{\partial \tilde{Q}_i} - \tilde{d}_i \int_{-\tilde{T}}^{\tilde{T}} d\tilde{\tau}' \frac{(\tilde{Q}_{i\tilde{\tau}} - \tilde{Q}_{i\tilde{\tau}'})}{(\tilde{\tau} - \tilde{\tau}')^2} = 0, \quad (\text{S25})$$

in which  $\tilde{m}_i, \tilde{d}_i$  reduces to  $M_i, D_i$  given in the main text when we impose the isotropic parameter choices  $m_i = m_0, d_i = d \sqrt{m_0 \mu_0}, \mu_i = \mu_0$ . From the next section on and also in the main text, we drop the tilde symbol for brevity. Note that this form is in the transformed monopole-centered  $\vec{Q}$  coordinate system. Without much loss of generality and to simplify the discussion henceforth, we will set in the original coordinate  $\vec{q}$  all parameters, including the mass  $\vec{m}$ , the dissipation strength  $\vec{d}$ , and the generated harmonic potential  $\vec{\mu}$ , isotropic but the spin Zeeman-like field  $\vec{w}$  and the effective coupling  $\vec{\alpha}$ . It describes effectively in the  $\vec{q}$ -space ( $\vec{Q}$ -space) that the instanton quasiparticle with (an)isotropic mass and dissipation moves under an anisotropic potential  $\tilde{V}$ , where  $\tilde{m}_i, \tilde{d}_i \propto \tilde{\alpha}_i^{-1}$ . Effectively, the  $\vec{Q}$ -space EOMs can be seen in each direction to have isotropic mass and dissipation but a force  $\tilde{\alpha}_i \partial \tilde{V} / \partial \tilde{Q}_i$ . Another choice would be setting  $\vec{m}, \vec{d}$  isotropic directly in the  $\vec{Q}$  space, which corresponds to the case where all parameters are isotropic but  $\vec{w}$  and  $\vec{\mu}$ . However, the instanton EOMs are still of the same type with isotropic mass and dissipation and a force  $\partial \tilde{V} / \partial \tilde{Q}_i$  instead and only insignificant quantitative difference can occur. All analytic and numerical discussions in this work are confirmed to hold in general.

## II. INSTANTON POTENTIAL LANDSCAPE

Let us now inspect the potential landscape  $V(\vec{Q})$ . Its extremum manifold is given by  $\frac{\partial V(\vec{Q})}{\partial Q_i} = \frac{2}{\alpha_i} (Q_i - w_i) - \frac{Q_i}{|\vec{Q}|} = 0$ . We have all  $\alpha_i > 0$ . To determine the nature of these extrema, we calculate the three eigenvalues  $\vec{\lambda} = (\lambda_1, \lambda_2, \lambda_3)$  or the principal minors of the Hessian matrix  $\frac{\partial^2 V}{\partial Q_i \partial Q_j}$ . Local minima are assured if all eigenvalues or all principal minors are positive.

Let us scan the whole positive octant in the 3D  $\vec{w}$ -space and assume  $\alpha_1 > \alpha_{2,3}$  without loss of generality.

1.  $\vec{w} = w_2\hat{2} + w_3\hat{3}$  (MQC)

Two degenerate local minima  $V_{\pm} = -(\frac{\alpha_1}{4} + \sum_{i=2,3} \frac{w_i^2}{\alpha_1 - \alpha_i})$  at  $\vec{Q}_{\pm} = (\pm\alpha_1\sqrt{\frac{1}{4} - \sum_{i=2,3} \frac{w_i^2}{(\alpha_1 - \alpha_i)^2}}, \frac{\alpha_1 w_2}{\alpha_1 - \alpha_2}, \frac{\alpha_1 w_3}{\alpha_1 - \alpha_3})$  that lie on the sphere  $|\vec{Q}| = \frac{\alpha_1}{2}$ . Using the principal minors of the Hessian, the necessary and sufficient condition for two local minima is  $\frac{1}{4} - \sum_{i=2,3} \frac{w_i^2}{(\alpha_1 - \alpha_i)^2} > 0$ . A simpler sufficient condition is  $\alpha_1 - \max[\alpha_2, \alpha_3] > 2|\vec{w}|$ . This corresponds to the MQC case referred in the main text.

2.  $\vec{w} = w_1\hat{1} + w_3\hat{3}$  (MQT)

Now we have  $\frac{2Q_2}{\alpha_2} = \frac{Q_2}{|\vec{Q}|}$ , which leads to  $|\vec{Q}| = \frac{\alpha_2}{2}$  or  $Q_2 = 0$ . Note that the former, same as the previous case up to an exchange of the coordinates 1 and 2, does not give two local minima under our assumption  $\alpha_1 > \alpha_{2,3}$ . Therefore, the only possibility left, the latter case with  $Q_2 = 0$ , gives two nondegenerate local minima at  $\vec{Q}_{\pm} = (w_1 + \frac{\alpha_1}{2} \cos \theta_{\pm}, 0, w_3 + \frac{\alpha_3}{2} \sin \theta_{\pm})$  where  $\theta_{\pm}$  takes two solutions from  $\frac{\cos \theta}{\sin \theta} = \frac{w_1 + \frac{\alpha_1}{2} \cos \theta}{w_3 + \frac{\alpha_3}{2} \sin \theta}$ , which amounts to a quartic equation with no concise form of roots. A simple sufficient condition is  $\alpha_1 - \alpha_3 > 4|\vec{w}|, \alpha_1 - \alpha_2 > 2|\vec{w}|$ .

3.  $\vec{w} = w_1\hat{1} + w_2\hat{2}$  (MQT)

Same as the previous case up to an exchange of the coordinates 2 and 3.

4.  $\vec{w} = w_1\hat{1} + w_2\hat{2} + w_3\hat{3}$  (MQT)

There is no simple analytic form of the position  $\vec{Q}_{\pm}$  of the two nondegenerate local minima. A simple sufficient condition is  $\alpha_1 - \max[\alpha_2, \alpha_3] > 4|\vec{w}|$ .

Next, we look into the case with  $\vec{w}$  aligned with one axis. Without loss of generality, we assume  $\vec{w} = w_3\hat{3}$  but do not put any restriction on  $\vec{\alpha}$ . There are three mutually exclusive cases.

1.  $\alpha_1 = \alpha_2$  continuous manifold of extrema(a)  $\alpha_1 = \alpha_2 = \alpha_3 = \alpha$ 

The solution is an  $S^2$ -sphere given by  $|\vec{Q}| = \alpha/2$ .

(b)  $\alpha_1 = \alpha_2 = \alpha_{12} \neq \alpha_3$ 

The solution is an  $S^1$ -ring given by  $|\vec{Q}| = \alpha_{12}/2, Q_3 = \frac{\alpha_{12}w_3}{\alpha_{12} - \alpha_3}$ .

2.  $\alpha_1 \neq \alpha_2$ (a)  $\alpha_1 \neq \alpha_3, Q_1 \neq 0$  (MQC)

The solution consists of two points  $\vec{Q}_{\pm} = (\pm\alpha_1\sqrt{\frac{1}{4} - (\frac{w_3}{\alpha_1 - \alpha_3})^2}, 0, \frac{\alpha_1 w_3}{\alpha_1 - \alpha_3})$  on the ring specified by  $|\vec{Q}| = \alpha_1/2, Q_2 = 0$  with  $\vec{\lambda} = (\frac{2}{\alpha_2} - \frac{2}{\alpha_1}, \frac{1}{\alpha_1\alpha_3}(\alpha_1 - \Delta), \frac{1}{\alpha_1\alpha_3}(\alpha_1 + \Delta)) > 0$  where  $\Delta = \sqrt{\frac{(\alpha_1 - 2\alpha_3)^2(\alpha_1 - \alpha_3) + 16\alpha_3 w_3^2}{\alpha_1 - \alpha_3}}$ . Under the necessary and sufficient condition  $\alpha_1 > \alpha_{2,3}, \alpha_1 - \alpha_3 > 2w_3$ , we have two degenerate minima  $V_{\pm} = -(\frac{\alpha_1}{4} + \frac{w_3^2}{\alpha_1 - \alpha_3})$  at  $\vec{Q}_{\pm}$  that lie symmetrically in the upper half of the  $Q_1Q_3$ -plane. We have a type-II Weyl crossing point[S48] when  $\alpha_3 < 2w_3$ . This matches the general discussion for  $\vec{w} = w_2\hat{2} + w_3\hat{3}$  and corresponds to the MQC case referred in the main text.

(b)  $\alpha_2 \neq \alpha_3, Q_1 = 0$  (MQC)

Same as the previous case up to an exchange of coordinate 1, 2.

3. (MQT) For general  $\vec{\alpha}$ , there is yet another solution  $\vec{Q}_{\pm} = (0, 0, w_3 \pm \frac{\alpha_3}{2})$ .  $\vec{\lambda} = (\frac{2}{\alpha_1} - \frac{2}{|\alpha_3 \pm 2w_3|}, \frac{2}{\alpha_2} - \frac{2}{|\alpha_3 \pm 2w_3|}, \frac{2}{\alpha_3}) > 0$ . Under the necessary and sufficient condition  $\alpha_3 - 2w_3 > \max[\alpha_1, \alpha_2] > 0$ , we have two nondegenerate local minima  $V_{\pm} = -|w_3 \pm \frac{\alpha_3}{2}| + \frac{\alpha_3}{4}$  at  $\vec{Q}_{\pm}$  and the conical crossing  $V_0 = \frac{w_3^2}{\alpha_3} > V_- > V_+$  at  $|\vec{Q}| = 0$ . If we instead set  $\vec{w} = w_1\hat{1}$  that means an exchange of the coordinates 1 and 3, it matches the general discussion for  $\vec{w} = w_1\hat{1} + w_3\hat{3}$  when  $\cos \theta = 0$  and corresponds to the MQT case referred in the main text.

### III. DETAILS IN SYMMETRY ANALYSIS

#### A. Time-reversed solutions

As noted in the main text for Table I, a pair of time-reversed paths of opposite gain and loss nature share the same total action. Let's show this by taking a look at the effective action Eq. (S11) as an example. While other

conventional terms are obviously invariant for the time-reversed path  $\vec{\sigma}(-\tau)$ , the temporally nonlocal  $\mathcal{S}_i$  in Eq. (S12) makes no exception

$$\begin{aligned}\mathcal{S}_i[\vec{\sigma}(-\tau)] &= \frac{1}{T} \int_{-T}^T d\tau d\tau' \sum_i \sigma_i(-\tau) \sigma_i(-\tau') K_i(\tau - \tau') = \frac{1}{T} \int_T^{-T} (-d\tau) (-d\tau') \sum_i \sigma_i(\tau) \sigma_i(\tau') K_i(\tau' - \tau) \\ &= \frac{1}{T} \int_{-T}^T d\tau d\tau' \sum_i \sigma_i(\tau) \sigma_i(\tau') K_i(\tau' - \tau) = \frac{1}{T} \int_{-T}^T d\tau' d\tau \sum_i \sigma_i(\tau') \sigma_i(\tau) K_i(\tau - \tau') = \mathcal{S}_i[\vec{\sigma}(\tau)].\end{aligned}\quad (\text{S26})$$

This is not surprising since the same conclusion holds as well with  $\vec{\sigma}(-\tau), \vec{q}(-\tau)$  for the equivalent and original action in Eq. (S8) that corresponds to Eq. (S1).

The system's energy at an instant of imaginary time is  $E(\tau) = \frac{1}{2} \sum_i m_i \dot{Q}_i^2 - V(\vec{Q})$ , which is certainly not conserved. Therefore, from Eq. (S25) the rate of energy variation is

$$\dot{E}(\tau) = \sum_i d_i \dot{Q}_i \int_{-T}^T dx' \frac{(Q_{i\tau} - Q_{i\tau'})}{(\tau - \tau')^2}.\quad (\text{S27})$$

Using these expressions, one can examine the gain and loss behavior of obtained instanton solutions.

### B. Mirror symmetry protection

The first line of Table II in the main text can be verified in Eq. (S25). In general, the instanton path  $\vec{Q}'(\tau)$  with energy gain, accompanied by the identical action as  $\vec{Q}(\tau)$  has, consists of  $Q_i(-\tau)$  in the  $i$ -direction when  $Q_i(-T) = Q_i(T)$  regardless of the existence of mirror symmetry  $\mathcal{M}_i$  and  $-Q_j(-\tau)$  in the  $j$ -direction when  $Q_j(-T) = -Q_j(T)$  and there is mirror symmetry  $\mathcal{M}_j$ . This complies with the general conditions for MQC in Sec. II and originates from the mirror symmetry  $\mathcal{M}_j$ . Note that one can translate and rotate the coordinate system to have  $Q_i(-T) = Q_i(T)$  in two directions and  $Q_j(-T) = -Q_j(T)$  in the other direction of two degenerate local minima. However, this alternative path  $\vec{Q}'(\tau)$  does not contribute to any interference effect to  $\vec{Q}(\tau)$ . Let's exemplify with two case discussed in Sec. II. For  $\vec{w} = w_1 \hat{1} + w_2 \hat{2}$ , since we have  $\cos \theta'(\tau) = -\cos \theta(-\tau)$  and  $\phi'(\tau) = -\phi(-\tau)$ , the Berry phase term  $\mathcal{S}_\Phi$  in Eq. (S3) differs only by an integral of the total derivative  $\dot{\phi}$ , which vanishes as dictated by the BC. The proof becomes even simpler for the equivalent but rotated case  $\vec{w} = w_2 \hat{2} + w_3 \hat{3}$  adopted in the main text, where  $\cos \theta'(\tau) = \cos \theta(-\tau)$ ,  $\phi'(\tau) = \phi(-\tau)$ . This absence of interference between  $\vec{Q}(\tau)$  and  $\vec{Q}'(\tau)$  is in a way an effect of the mirror symmetry.

Nonetheless, while the above discussion still holds, the situation alters when there is one mirror symmetry more. For an instanton solution  $\vec{Q}(\tau)$ , there can be another equally possible instanton path  $\vec{Q}^r(\tau)$  that differs in the  $i$ -direction by  $-Q_i(\tau)$  as a solution to Eq. (S25) when  $Q_i(-T) = Q_i(T) = 0, \alpha_j > \alpha_{i,k}$  and there are two mirror symmetries  $\mathcal{M}_i, \mathcal{M}_j$  with mutually unequal  $\alpha_{i,j,k}$ . Note that one cannot arbitrarily translate the coordinate system to accommodate this special boundary position since the quadratic and monopolar potentials in Eq. (S24) in general have distinct inversion centers when  $\vec{w} \neq 0$ . For instance, when  $\vec{w} = w \hat{3}$  as discussed in Sec. II, one has mirror symmetries  $\mathcal{M}_1, \mathcal{M}_2$ . Any instanton path  $\vec{Q}(\tau)$  also has a symmetry related pair  $\vec{Q}^r(\tau) = \mathcal{M}_2 \vec{Q}(\tau) = (Q_1(\tau), -Q_2(\tau), Q_3(\tau))$  as another path connecting the endpoints related by  $\mathcal{M}_1$ , which gives  $\cos \theta^r(\tau) = \cos \theta(\tau), \phi^r(\tau) = -\phi(\tau)$  and hence a reversed Berry phase factor  $\Phi^r = -\Phi$  where  $\Phi$  is for  $\vec{Q}(\tau)$ . In the absence of the extra mirror symmetry, there is only one single instanton path  $\vec{Q}(\tau)$  and its pair  $\vec{Q}^r(\tau)$  with no phase difference. Now the MQC tunnel amplitude is calculated as shown in the main text, where we have used the fact that  $\mathcal{S}_Q[\vec{Q}(\tau)] = \mathcal{S}_Q[\vec{Q}^r(\tau)] \equiv \mathcal{S}_Q, \mathcal{S}_\Phi[\vec{Q}(\tau)] = -\mathcal{S}_\Phi[\vec{Q}^r(\tau)] \equiv \mathcal{S}_\Phi = -\mathcal{S}_\Phi^* = i\Phi$ . The MQC tunnel splitting  $\Delta \propto A_0$ , which can be seen from Eq. (S33).

## IV. NUMERICAL METHOD

We provide some comments and the details of our approach to the BVP of a system of nonlinear integro-differential equations with a Fredholm integral. Firstly, any BVP is fundamentally distinct from the initial value problem (IVP). An IVP of classical particle scattering has been discussed in the presence of monopolar field[S49]. Secondly, this BVP cannot be converted into an ordinary differential equation (ODE) problem by differentiating the system and linear integral transforms like the Laplace transform are of no use. Thirdly, there are in principle other methods one may resort to. In an iterative method one replaces the unknown function in the integrand by the solution from the previous round or by an ansatz or guess when it is the first round, and then solves the resulting ODE repeatedly until

convergence. Besides, one can also conceptually approximate the solution by a polynomial of a certain degree and thus justify differentiating the system enough times and dropping the Fredholm integral, then followed by shooting methods for BVP for instance. Other possibilities may include differential transform method[S35], Chebyshev decomposition method[S36], and various asymptotic techniques[S37]. However, in the methods above, the procedure is sometimes not well-controlled and may heavily depend on the initial guess due to nonlinearity: hardship in achieving correct convergence significantly augments the computational cost.

Here, we solve this problem efficiently combining the finite difference method (FDM)[S36, S38] and the Gaussian quadrature rule[S40].

- The Gaussian quadrature rule with  $n$  points helps evaluate the integral as a weighted sum based on a class of orthogonal polynomials and is accurate for polynomial integrands of degree  $2n - 1$  or less. Here, as the integrand is free from endpoint singularities and integrated over a finite region, we adopt the Gauss-Legendre quadrature using Legendre polynomials. We use finite but large enough range of imaginary time  $[-T, T]$  to assure convergence of the solution. The quadrature grid nodes are the roots  $x_i$  of the Legendre polynomial  $P_n(x)$  and the weights are given by  $w_i = \frac{2}{(1-x_i^2)P'_n(x_i)}$ . The change of integration interval is given by  $\int_a^b f(x)dx = \frac{b-a}{2} \int_{-1}^1 f\left(\frac{b-a}{2}\xi + \frac{a+b}{2}\right) d\xi$ . The grid nodes and weights can be generated using the Golub-Welsch algorithm[S50] or the Laurie's algorithm[S51] based on the positive-definite real symmetric Jacobi matrix. Both the differentiation and integration are processed as per the grid from the Gauss-Legendre quadrature as the integral requires more careful and stringent discretization than the equally spaced Newton-Cotes rules while the differentiation is less susceptible.
- We do not utilize adaptive quadratures with refined subdivisions as we intend to solve the integro-differential equation system at once in an FDM manner. This, however, requires generic generation of finite difference formulae on arbitrary grids, i.e., nonuniform or irregular stencils. Generic finite difference formulae are equivalent to derivatives of Lagrange interpolating polynomials, for which Taylor expansion is exact. In general, a finite difference formula of  $t$ -th order derivative on  $s$ -point data has at least asymptotic order  $s - t$  for the error reduction and is exact for polynomials of degree  $s - 1$ . The approximation is better on uniform grids with centered differences. Here, we can use Fornberg's efficient recursion algorithm for finite difference weights on irregular stencils based on polynomial interpolation[S39]. We apply (partially) one-sided forward or backward formulae near the edges and centered formulae in the bulk. As our problem bears no Gibb's oscillation, a good balance between numerical roundoff error and systematic approximation error is achieved using fourth-order differences, i.e., asymptotic order of error reduction  $O(h^4)$ .
- Consequently, the system of three nonlinear integro-differential equations is converted to a system of  $3m$  nonlinear algebraic equations of  $3m$  unknowns where  $m = n + 2$  is the number of grid points in each of the three dimensions including the two endpoints left out in the Gaussian quadrature rule. To express the BVP, we replace the leftmost and the rightmost equations by the Dirichlet BCs specified at the edges. This set of nonlinear algebraic equations can be solved efficiently by root-finding algorithms with one or more initial guesses, e.g., Newton's method and Brent's hybrid method[S41, S42]. The crudest initial guess can be a constant function. Better and faster solutions can be readily facilitated by using an earlier solution as the initial guess. This earlier solution can be one solved with less grid points and especially one that breaks a certain symmetry and thus certainly helps reach the distinct symmetry-related instanton paths. For the sake of further analysis of the instanton paths, any discrete solution obtained can be used to construct a continuous and differentiable function by cubic spline interpolation[S41, S42].

## V. ANALYTICAL ANALYSIS OF INSTANTON SOLUTIONS

We provide some analytical analysis to understand the behavior of the instantons in the phase diagram in the main text where we have  $\vec{w} = w\hat{z}$ .

- $w = 0$ 
  - $\alpha_1 > \alpha_2 > \alpha_3$  This directly corresponds to the calculation shown in the main text. The instanton path must lie in the  $Q_1Q_2$ -plane, because one can rotate, with respect to the  $Q_1$ -axis, any path with finite  $Q_3$  component into the  $Q_1Q_2$ -plane as per the homogeneous BCs in  $Q_{2,3}$  and achieve a smaller action in Eq. (S23), which holds regardless of the strength of the dissipation. Therefore, the instanton paths always

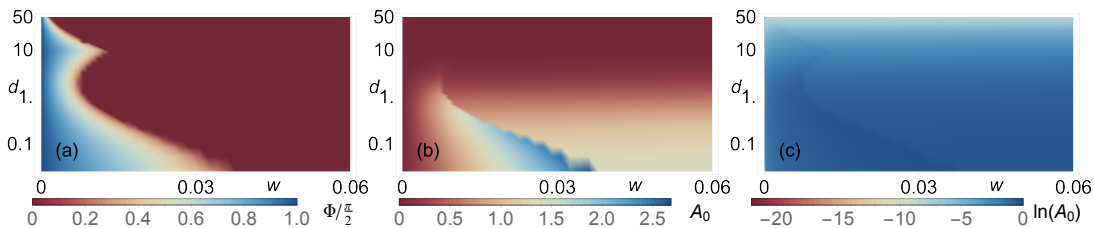


FIG. S1. Phase diagrams of (a) instanton Berry phase  $\Phi$  and (b) coherent tunnel amplitude  $A_0$  and (c) logarithmic scaled  $\ln A_0$  against potential bias  $w$  and logarithmic scaled dissipation strength  $d$ . Instantons are solved with settings same as Fig. 2 in the main text, scanning a  $50 \times 50$ -mesh of the  $wd$ -plane that is denser for smaller  $d$ .

come with full topological suppression due to  $\Phi = \pi/2$  as long as the system spontaneously exhibits finite  $Q_2$ , which is what one observes up to very large  $d$  as shown in Fig. S1.

- $\alpha_1 > \alpha_3 > \alpha_2$  Same as the previous one up to an exchange of coordinate 2, 3 as one has both  $\mathcal{M}_2$  and  $\mathcal{M}_3$  mirror symmetries.

- $w > 0$

- $\alpha_1 > \alpha_2 > \alpha_3$  This directly corresponds to the calculation shown in the main text. The previous rotation argument no longer applies since finite  $w$  renders a rotated path not fulfilling the instanton's inhomogeneous BC in  $Q_3$ . Therefore, the instanton path will acquire a finite  $Q_3$  component. While the instanton alters to be restricted in the  $Q_1Q_3$ -plane outside the critical curve  $f$ , it is in general *not* within any certain 2D plane inside  $f$  as mentioned in the main text, which is consistent with the nonconservation of angular momentum due to the noncentral force from  $V$  in Eq. (S25). This is also verified in the numerical solutions using the least square matrix eigenvalues of points along an instanton path, although barely discernible in Fig. 3 in the main text. Also note that  $\alpha_2 = \alpha_3$  bears a degenerate minima ring as aforementioned in Sec. II, invalidating the double-minima discussions so far. Indeed, as  $\alpha_2 \rightarrow \alpha_3 + 0^+$ , any  $Q_2 \neq 0$  path eventually disappears and the critical curve  $f$  shrinks inwards, which connects to the following case.
- $\alpha_1 > \alpha_3 > \alpha_2$  Paths with finite  $Q_2$  are not energetically favourable and because of the finite  $w_3$ , there is only one single intanton path in the upper  $Q_1Q_3$ -plane and thus  $\Phi = 0$ .

For the region of larger  $d$  not comparable to other system parameters, the phase boundary curve  $f$  possesses a complex shape, because within the finite phase region inside  $f$ ,  $\Phi(w > 0, d)$  does not vary monotonically with  $d$ , as shown in Fig. S1(a). At finite but not too large  $w$ , it first decreases until a stationary point, then increases until a second stationary point, and finally decreases to zero. Instead of having the first stationary point, for slightly larger  $w$  it may show an intermediate region of  $\Phi = 0$  at not too large  $d$ , which means an inflection point and a convex hump with cusp outward on the  $f$  curve. Usually, for  $d$  beyond this inflection point higher than  $d = 1$ , the instanton solution begins to deform and, dependent on a certain direction's BC is parity even or odd, asymptotically approach in that direction a  $\mathcal{T}$ -symmetric or  $\mathcal{T}$ -antisymmetric form without net energy change, as the nonlocal interaction term eventually outweighs the potential  $V$  in Eq. (S25). On the other hand, for larger and larger  $w$  beyond  $f$  and towards the edge of the MQC condition  $w = (\alpha_2 - \alpha_3)/2$  mentioned in the main text, the BC dictates that the range roved by an instanton reduces towards zero and stays local and high in the  $Q_1Q_3$ -plane relative to the monopole at the origin. Within the instanton path, the potential  $V$  thereby barely varies around the minimum value. Again, we are led to have the potential  $V$  suppressed and asymptotically reach  $\mathcal{T}$ -(anti)symmetric behavior.

To understand this inclination towards (anti)symmetrization, we can thus consider Eq. (S25) without the potential term, which has a linear integro-differential operator of even parity. This means that from any solution  $Q_i(\tau)$  in the  $i$ -direction one can construct parity even/odd solutions  $Q_i^{e/o}(\tau) = (Q_i(\tau) \pm Q_i(-\tau))/2$ , which can all be made consistent with the even/odd BCs in  $Q_3/Q_1$  while  $Q_2$  satisfies both. From the linearity and the physical nature, the uniqueness of solution guarantees  $Q_3(\tau)/Q_1(\tau)$  is even/odd and  $Q_2$  is parity definite or zero. This holds even when the kinetic term is also negligible. However, it is never legitimate to completely drop the potential term, otherwise the three components  $Q_{1,2,3}$  are totally decoupled and one is left with trivial solutions, i.e., the potential  $V$  is in a way nonperturbative to the system. The competition due to larger  $d$  between the nonlinear  $V$  and the trend of (anti)symmetrization generates the complex phase boundary with the cusped hump structure, although eventually at large enough  $d$  the phase  $\Phi$  will tend to zero at any finite  $w$  as shown.

Across the phase boundary  $f$  curve in Fig. S1(a), the corresponding  $A_0$ -jump always exists, although it eventually gets smoothed out at large enough  $d$  since large enough  $\mathcal{S}_Q$  exponentially suppresses the jump, as shown in Fig. S1(b). To reassure us about this phase transition with jump, we show a logarithmic plot in Fig. S1(c), where the jump becomes more visible. In summary, beyond the phase diagram in the main text, for larger  $d$  that is less and less comparable to  $m, w, \bar{\alpha}$  typically equal or less than unity,  $\Phi$  can vary nonmonotonically although eventually vanishes. The complexities originate from that when potential  $V$  becomes less important the remaining parity-even linear integro-differential operator causes the instanton to (anti)symmetrize in  $\tau$ , although  $V$  is still crucial to nonlinearly couple three directions. We describe here this large- $d$  behavior for completeness, probably of less physical interest as the modelling could become less reliable towards realistic situations.

## VI. DISSIPATIVE INSTANTON GAS TUNNELLING

One might generalize the instantons discussed so far to a 1D dissipative instanton gas with multiple instantons and interaction as well. For instance, although dissipation has been included in the action of single instantons, it still exists between instanton events at different times, which gives a 1D logarithmic interaction  $C_{ij}(|\tau_i - \tau_j|) = -c_{ij} \ln |\tau_i - \tau_j|$  in the dilute limit[S46]. Incorporating this between (anti)instantons leads to the grand-canonical partition function, the total transition amplitude from  $\bar{Q}_-$  to  $\bar{Q}_+$  or back to  $\bar{Q}_-$  is given by

$$\begin{aligned} A(\bar{Q}_-, \bar{Q}_\mp) &= \mathcal{Z}_{\text{IG}} = \sum_{n=0}^{\infty} \sum_{\{p_i=\pm 1, \xi_i=\pm 1\}} \int_{-T}^T d\tau_1 \int_{-T}^{\tau_1} d\tau_2 \cdots \int_{-T}^{\tau_{n+m-1}} d\tau_{n+m} e^{-[\sum_{i<j}^{n+m} q_i q_j C_{ij}(|\tau_i - \tau_j|) + \sum_i (\mathcal{S}_Q + i q_i \xi_i \Phi)]} \\ &= \sum_{n=0}^{\infty} \int_{-T}^T d\tau_1 \int_{-T}^{\tau_1} d\tau_2 \cdots \int_{-T}^{\tau_{n+m-1}} d\tau_{n+m} y^{n+m} e^{-[\sum_{i<j}^{n+m} q_i q_j C(|\tau_i - \tau_j|)]}, \end{aligned} \quad (\text{S28})$$

where  $m = n + \frac{1-\mp 1}{2}$ , the charges  $\xi_i = \pm 1, p_i = \pm 1, q_i = (-1)^{i+1}$  denote for the  $i$ th instanton respectively whether it is  $\bar{Q}^r$  instanton, whether it is  $\bar{Q}'$  instanton although this does not affect the single-instanton action directly, and the direction of motion (instanton/antiinstanton). In principle, instanton events centered at  $\tau_i$  and  $\tau_j$  could have their interaction coefficient  $c_{ij}$  dependent on the respective instanton type (among the possible four) as the overlap integral differs, i.e., dependent on the charges  $\xi_i, p_i$ , hence the subscript of  $c_{ij}$ . In this case, the summation in the first line of Eq. (S28) renders the fugacity inseparable from the interaction, which is a more complex instanton gas than usual cases like the Kondo analogy in the main text.

In the dilute limit, assuming that the instanton interaction does not depend on the charges  $\xi_i, p_i$ , i.e.,  $c_{ij} = c$ , one can perform the summation on the gas fugacity due to the instanton core energy as shown in the second line of Eq. (S28), leading to  $y = 2K e^{-\mathcal{S}_{\text{core}}}$  with  $\mathcal{S}_{\text{core}} = \mathcal{S}_Q - \ln(2 \cos \Phi)$  (see the noninteracting case below). An interacting neutral Coulomb gas can be mapped to the sine-Gordon model. However, the reverse procedure is not applicable here since the time ordering of the instantons is in general unremovable. In other words, the failure partially lies in the invalidity of the following transformation  $\int_{-T}^T d\tau_1 \int_{-T}^{\tau_1} d\tau_2 \cdots \int_{-T}^{\tau_{n+m-1}} d\tau_{n+m} f(|\tau_i - \tau_j|) \neq \frac{1}{n!m!} \int_{-T}^T d\tau_1 \int_{-T}^{\tau_1} d\tau_2 \cdots \int_{-T}^{\tau_{n+m}} d\tau_{n+m} f(|\tau_i - \tau_j|)$  where  $f(|\tau_i - \tau_j|)$  denotes a generic function dependent on all possible  $|\tau_i - \tau_j|, i \neq j$ . Instead, it formally resembles the anisotropic Kondo problem. In this regard,  $c = 2\mathcal{K}$  where  $\mathcal{K} = d[2Q_1(T)]^2/2$  determines whether the system flows to localization ( $\mathcal{K} > 1$ ) or not ( $\mathcal{K} < 1$ ) and  $\mathcal{K} = 1/2$  is the Toulouse limit[S8]. To see this, in the anisotropic Kondo model

$$\mathcal{H}_{\text{AK}} = v_F \sum_{k,\sigma} k c_{k\sigma}^\dagger c_{k\sigma} + J_{\parallel}/4 s_z \sum_{\sigma} \sigma c_{\sigma}^\dagger c_{\sigma} + J_{\perp}/2 (s_+ c_{\downarrow}^\dagger c_{\uparrow} + s_- c_{\uparrow}^\dagger c_{\downarrow}) \quad (\text{S29})$$

we would have  $y = \rho J_{\perp}/2, \mathcal{K} = (1 - \rho J_{\parallel}), \rho = 1/2\pi v_F$ , where  $\vec{s}$  is the localized spin. And the renormalization group equations are to the lowest order

$$\begin{aligned} d(1 - \mathcal{K})/d \ln \tau_c &= \mathcal{K} y^2/4 \\ dy/d \ln \tau_c &= (1 - \mathcal{K})y \end{aligned} \quad (\text{S30})$$

where  $1/\tau_c$  denotes the running high-energy cutoff.

We now consider the case of a noninteracting dissipative dilute instanton gas in more details. By taking into account all possible numbers and configurations of instantons,

$$A(\vec{Q}_-, \vec{Q}_\mp) = \sum_{n=\text{even/odd}} K^n \int_{-T}^T d\tau_1 \int_{-T}^{\tau_1} d\tau_2 \cdots \int_{-T}^{\tau_{n-1}} d\tau_n A_n(\tau_1, \cdots, \tau_n) \quad (\text{S31})$$

where the fluctuation determinant  $K$  is a prefactor of the exponential amplitude  $A_n$  and can be calculated by taking into account the possible Goldstone mode in  $\tau$ -space[S16, S17, S52]. We do not evaluate  $K$  here as it does not affect the exponential accuracy that we are mainly interested in. The transition amplitude  $A_n = A_n^{\text{inst}} A_n^{\text{flct}}$  with  $n$  (anti)instantons consists of two parts. The instanton part

$$A_n^{\text{inst}}(\tau_1, \cdots, \tau_n) = \sum_{\{p_i=\pm 1, \xi_i=\pm 1\}} \prod_i e^{-(S_Q + i\xi_i q_i \Phi)} = e^{-nS_Q} \prod_i \sum_{p_i=\pm 1, \xi_i=\pm 1} e^{-i\xi_i q_i \Phi} = (4e^{-S_Q} \cos \Phi)^n = A_0^n. \quad (\text{S32})$$

The quantum fluctuation part accounts for the harmonic fluctuation accumulated while sitting at the minima  $A_n^{\text{flct}} = \prod_i e^{-\omega(\tau_{i+1}-\tau_i)/2} = e^{-\omega T}$  wherein  $\omega$  is frequency determined by the harmonic potential approximation  $m\omega^2 = V''(\vec{Q}_\pm)$ [S53]. Therefore, we have

$$\begin{aligned} A(\vec{Q}_-, \vec{Q}_\mp) &= B \sum_{n=\text{even/odd}} K^n e^{-\omega T} A_0^n \int_{-T}^T d\tau_1 \int_{-T}^{\tau_1} d\tau_2 \cdots \int_{-T}^{\tau_{n-1}} d\tau_n \\ &= B e^{-\omega T} \sum_{n=\text{even/odd}} \frac{1}{n!} (2KT A_0)^n = B e^{-\omega T} \begin{cases} \cosh(2KT A_0) & n = \text{even} \\ \sinh(2KT A_0) & n = \text{odd} \end{cases}. \end{aligned} \quad (\text{S33})$$

Prefactor  $B$  is introduced to account for the state overlap with the spontaneously formed even/odd state  $|e/o\rangle$ , i.e.,  $\langle \vec{Q}_+ | e \rangle = \langle \vec{Q}_- | e \rangle$ ,  $\langle \vec{Q}_+ | o \rangle = -\langle \vec{Q}_- | o \rangle$ , and  $B/2 = |\langle \vec{Q}_\mp | e/o \rangle|^2$ . It can then be compared to the same quantity calculated from the  $|e/o\rangle$  state splitting

$$A(\vec{Q}_-, \vec{Q}_\mp) = \langle \vec{Q}_- | (e^{-(\omega-\Delta)T} |e\rangle \langle e| + e^{-(\omega+\Delta)T} |o\rangle \langle o|) | \vec{Q}_\mp \rangle, \quad (\text{S34})$$

from which we obtain the tunnel splitting  $\Delta = K A_0$ .